

Many-objective New Bat Algorithm and Constraint-Priority Non-inferior Sorting Strategy for Optimal Power Flow

Gonggui Chen, Jie Qian, Zhizhong Zhang*, and Zhi Sun

Abstract—Non-convex property and huge computation of multi-objective optimal power flow (MOOPF) problems make it unsuitable to be solved by traditional approaches. A many-objective new bat (MONBA) algorithm which improves the speed updating and local searching models is proposed in this paper to handle the MOOPF problems. Moreover, an efficient constraint-priority non-inferior sorting (CPNS) strategy is put forward to seek the satisfactory-distributed Pareto Frontier (PF). Six simulation trials aimed at optimizing the power loss, emission and fuel cost are performed on the IEEE 30-node, 57-node and 118-node systems. In contrast to the classical NSGA-II and many-objective basic bat (MOBBA) algorithms, the great edges of presented MONBA-CPNS algorithm in solving the MOOPF problems are powerfully validated. In addition, two performance criteria, which can intuitively measure the distribution and convergence of obtained Pareto optimal set (POS), provide more compelling proof for the superiority of MONBA-CPNS algorithm.

Index Terms—Many-objective new bat algorithm, Optimal power flow, Non-inferior sorting strategy, Performance criteria

I. INTRODUCTION

THE optimal power flow (OPF) is an indispensable means to realize the economic operation of electric systems [1-3]. The study of OPF problem aims to minimize the power loss or fuel cost, separately [4, 5]. However, the single-object optimization has some limitations due to the diverse demands of users.

The multi-objective optimal power flow (MOOPF) problems, which take more than one goals into consideration at the same time, have been favored by many scholars.

Manuscript received June 25, 2019; revised September 20, 2019. This work was supported by the National Natural Science Foundation of China (Nos. 51207064 and 61463014).

Gonggui Chen is with the Key Laboratory of Industrial Internet of Things & Networked Control, Ministry of Education, Chongqing University of Posts and Telecommunications, Chongqing 400065, China; Key Laboratory of Complex Systems and Bionic Control, Chongqing University of Posts and Telecommunications, Chongqing 400065, China (e-mail: chenggpower@126.com).

Jie Qian is with the Key Laboratory of Industrial Internet of Things & Networked Control, Ministry of Education, Chongqing University of Posts and Telecommunications, Chongqing 400065, China (e-mail: qianjie@126.com).

Zhizhong Zhang is with the Key Laboratory of Communication Network and Testing Technology, Chongqing University of Posts and Telecommunications, Chongqing 400065, China (corresponding author, Tel: 023-62461681; e-mail: zhangztx@163.com).

Zhi Sun is with the Chn Energy Enshi Hydropower Co., Ltd, Enshi 445000, China (e-mail: sunzhi24@126.com).

Essentially, the MOOPF problem with non-differentiable property is a mathematical model for minimizing the given optimization objectives [6-8].

Intelligent algorithms play an important role in solving the MOOPF problems. Until now, the modified bio-inspired algorithm [9], the quasi-oppositional modified Jaya algorithm [10] and the multi-objective firefly algorithm [11] have successfully solved the MOOPF problems.

The original and improved bat algorithms with easily-adjustable parameters have great potential to deal with various practical problems such as the data clustering problem [12], the goods distribution problem [13] and the wireless sensor network deployment [14]. It is a pity the many-objective basic bat (MOBBA) algorithm may encounter some problems such as poor-diversity and premature-convergence when dealing with the MOOPF problems. Thus, two improved updating modes based on the difference of *Rank* index are proposed to reconstitute the many-objective new bat (MONBA) algorithm. For elite individuals, that is, the individuals with *Rank*=1, a nonlinear adjustment factor is integrated into the speed term to improve the population-variability. For the non-elite ones, the location is updated by generating a random disturbance near the elite individuals.

Furthermore, in order to select the high-quality Pareto optimal set (POS), an effective constraint-priority non-inferior sorting (CPNS) strategy is presented in this paper. The advantage of CPNS strategy is that, it can pick out the satisfactory POS that do not violate any system constraints without any additional parameters. Combining two above contributions, the innovational MONBA-CPNS method is put forward to handle the non-differentiable MOOPF problems.

The structure of this paper is summarized as follows. The optimal objects and restrained conditions of MOOPF model are given in Section II. The improvements of MONBA algorithm and the novel CPNS sorting strategy are introduced in Section III. Besides, Section III gives the main steps of MONBA-CPNS algorithm in dealing with the MOOPF problems. Six simulation experiments and the detailed results analysis are given in Section IV and Section V, respectively. The conclusion is made in Section VI eventually.

II. MATHEMATICAL DESCRIPTION

The mathematic model of MOOPF problems includes multiple object functions and restrained conditions. In this paper, the former part involves the emission *OE*, the fuel cost *OF*, the power loss *OP* and the fuel cost with value-point

effect OF_v . The latter part is composed by equality constraints which reveal power balance and inequality ones which limit the valid ranges of electrical equipment.

A. Optimal Objects

The objective functions of OE , OF , OP and OF_v are defined as follows [15, 16].

- OE minimization

$$OE = \sum_{i=1}^{N_G} [\alpha_i P_{Gi}^2 + \beta_i P_{Gi} + \gamma_i + \eta_i \exp(\lambda_i P_{Gi})] \text{ ton/h} \quad (1)$$

- OF minimization

$$OF = \sum_{i=1}^{N_G} (a_i + b_i P_{Gi} + c_i P_{Gi}^2) \text{ \$/h} \quad (2)$$

- OP minimization

$$OP = \sum_{k=1}^{N_l} g_k [V_i^2 + V_j^2 - 2V_i V_j \cos(\delta_i - \delta_j)] \text{ MW} \quad (3)$$

- OF_v minimization

$$OF_v = \sum_{i=1}^{N_G} (a_i + b_i P_{Gi} + c_i P_{Gi}^2 + |d_i \times \sin(e_i \times (P_{Gi}^{\min} - P_{Gi}))|) \text{ \$/h} \quad (4)$$

B. Restrained Conditions

The restrictions of power systems can be divided into the equality constraints and inequality ones.

1) Equality Constraints

$$P_{Gi} = P_{Di} + V_i \sum_{j \in N_l} V_j (G_{ij} \cos(\delta_i - \delta_j) - B_{ij} \sin(\delta_i - \delta_j)) \quad (5)$$

$$i \in N$$

$$Q_{Gi} = Q_{Di} + V_i \sum_{j \in N_l} V_j (G_{ij} \sin(\delta_i - \delta_j) + B_{ij} \cos(\delta_i - \delta_j)) \quad (6)$$

$$i \in N_{PQ}$$

2) Inequality Constraints

The formulas (7) ~ (10) show the inequality constraints on state variables while formulas (11) ~ (14) show the inequality constraints on control variables. The specific meanings of involved parameters are clarified in literatures [6, 15].

- Generator active power at slack bus P_{G1}

$$\begin{aligned} P_{G1}^{\max} - P_{G1} &\geq 0 \\ P_{G1} - P_{G1}^{\min} &\geq 0 \end{aligned} \quad (7)$$

- Voltages at load buses V_L

$$\begin{aligned} V_{Li}^{\max} - V_{Li} &\geq 0 \\ V_{Li} - V_{Li}^{\min} &\geq 0 \end{aligned}, i \in N_{PQ} \quad (8)$$

- Generator reactive power Q_G

$$\begin{aligned} Q_{Gi}^{\max} - Q_{Gi} &\geq 0 \\ Q_{Gi} - Q_{Gi}^{\min} &\geq 0 \end{aligned}, i \in N_G \quad (9)$$

- Apparent power S

$$S_{ij}^{\max} - S_{ij} \geq 0, ij \in N_L \quad (10)$$

- Generator active power P_G

$$\begin{aligned} P_{Gi}^{\max} - P_{Gi} &\geq 0 \\ P_{Gi} - P_{Gi}^{\min} &\geq 0 \end{aligned}, i \in N_G (i \neq 1) \quad (11)$$

- Voltages at generation buses V_G

$$\begin{aligned} V_{Gi}^{\max} - V_{Gi} &\geq 0 \\ V_{Gi} - V_{Gi}^{\min} &\geq 0 \end{aligned}, i \in N_G \quad (12)$$

- Transformer tap-settings T

$$\begin{aligned} T_i^{\max} - T_i &\geq 0 \\ T_i - T_i^{\min} &\geq 0 \end{aligned}, i \in N_T \quad (13)$$

- Reactive power injection Q_C

$$\begin{aligned} Q_{Ci}^{\max} - Q_{Ci} &\geq 0 \\ Q_{Ci} - Q_{Ci}^{\min} &\geq 0 \end{aligned}, i \in N_C \quad (14)$$

III. OPTIMAL STRATEGIES

The modified MONBA algorithm and the novel CPNS sorting strategy which are conducive to handle the complex MOOPF problems are presented.

A. MOBBA Algorithm

The MOBBA method combining the basic bat algorithm and the multi-objective Pareto dominated strategy is capable to handle the MOOPF problems.

The location Lo of basic bat algorithm is updated by the speed Sp and frequency Fr items [17]. The mathematical expressions of three above parameters are defined as follows. For MOOPF problems, the Lo and Sp are essentially D -dimensional adjustable control variables of power system.

$$Fr(i) = Fr_{\min} + \mu_1 * (Fr_{\max} - Fr_{\min}) \quad (15)$$

$$Sp_i(t) = Sp_i(t-1) + Fr(i) * (Lo_i(t-1) - Lo_{best}) \quad (16)$$

$$Lo_i(t) = Lo_i(t-1) + Sp_i(t) \quad (17)$$

where u_1 ($u_1 \in (0,1)$) represents a random constant and Lo_{best} indicates the best individual so far. The valid range of frequency is set as $[Fr_{\min}, Fr_{\max}]$.

The local search operation, which is helpful to explore a higher-performance scheme near the Lo_{best} individual, will be performed after updating the locations of all bat individuals. For local operation, the loudness intensity lou and pulse rate pul are mathematically as formulas (18) and (19) [17, 18].

$$lou_i(t+1) = l_1 * lou_i(t) \quad (18)$$

$$pul_i(t+1) = pul_0 (1 - \exp(-l_2 t)) \quad (19)$$

where l_1 ($l_1 \in (0,1)$) and l_2 ($l_2 > 0$), respectively, indicate the attenuation and increase coefficients of two local parameters.

Combined the Pareto dominate rule, MOBBA algorithm can basically deal with the MOOPF problems. However, there are some shortcomings for the MOBBA-CPNS method such as long running time and poor performance of best compromise solution (BCS). Consequently, the modified MONBA-CPNS algorithm which can effectively overcome the mentioned defects is proposed in this paper.

B. MONBA Algorithm

The MONBA algorithm mainly improves the performance of MOBBA algorithm in solving MOOPF problems from the two following perspectives.

1) Integration of Weight Coefficient

In order to explore the potential solutions with satisfactory variability, a nonlinearly-adjusted weight coefficient We is introduced into the renewing of Sp . The definitions of We and novel speed model are shown as formulas (20) and (21).

$$We(t+1) = We_{\max} - \mu_2 * Wd + u_3 * (We(t) - Ws / 2)$$

$$\begin{cases} Wd = We_{\max} - We_{\min} \\ Ws = We_{\max} + We_{\min} \end{cases} \quad (20)$$

$$Sp_i(t) = We(t) Sp_i(t-1) + u_4 Fr(i) (Lo_{best} - Lo_i(t)) \quad (21)$$

where $u_2 \sim u_4$ ($u_2 \sim u_4 \in (0,1)$) are random constants while the We coefficient is limited within $[We_{min}, We_{max}]$.

2) Simplification of Local Search

For MOBBA method, the local search will be conducted when condition (22) is satisfied.

$$\begin{cases} pul_i < u_5 \\ lou_i > u_6 \\ Lo_{new} \text{ do min ates } Lo_{best} \end{cases} \quad (22)$$

where u_5 and u_6 are two different constants which belong to $(0,1)$. The Lo_{new} is a new individual randomly generated near the Lo_{best} one.

The dominant relationship of two power flow solutions is judged based on the values of constraint-violation and objectives. In detail, the i th solution has a predominant capability to the j th one when condition (23) or (24) is met.

$$cons(Lo_i) < cons(Lo_j) \quad (23)$$

$$\begin{cases} cons(Lo_i) = cons(Lo_j) \\ O_m(Lo_i) \leq O_m(Lo_j), \forall m \in \{1, 2, \dots, M\} \\ O_n(Lo_i) < O_n(Lo_j), \exists n \in \{1, 2, \dots, M\} \end{cases} \quad (24)$$

where $cons(Lo_i)$ is the constraint-violation value of the i th solution and $O_m(Lo_i)$ indicates the corresponding m th objective value of the i th solution. M is the amount of objectives for synchronous optimization.

However, the local search unavoidably takes more computation time. To enhance the search efficiency, the potential individuals of MONBA algorithm are divided into two parts. One is the elite population (EP) and the other is non-elite population (NEP). The EP and NEP populations will adopt different modes to update their locations. The individuals of EP population renovate their information based on the formulas (21) and (17) while the ones of NEP population renovate themselves by producing disturbance to a randomly-selected elite individual.

C. CPNS Strategy

The CPNS strategy is proposed to select the Nr high-quality Pareto solutions from the candidate population (CP) with Nc solutions. The CP population is generated by combining the initial population (IP) and remained population (RP). In particular, the IP population of MOOPF problems is obtained based on formula (25). The POS set obtained by the i th iteration will be the RP population of the $(i+1)$ th iteration.

$$Lo_i = u^{\min} + \zeta(u^{\max} - u^{\min}), i = 1, 2, \dots, Nr \quad (25)$$

where u^{\min} and u^{\max} are the lower and upper bounds of D -dimensional control variables. The ζ ($\zeta \in (0,1)$) is a random constant.

The rank ($Rank$) and the crowding distance ($Cdis$) characteristics of CPNS strategy can be determined as follows.

1) Rank Index

Referring to the sorting approach proposed by Deb [19, 20], the key to obtain the $Rank$ index of each solution in CP population is summarized as three steps.

i) Find the solutions which are not dominated by all the rest of solutions in CP population and assign them as $Rank=1$. The solutions with $Rank=1$ are the mentioned elite individuals.

ii) Disregard these solutions with $Rank=1$ and determine

another solution set which is not dominated by other solutions based on the dominance rule shown as formulas (23) and (24). The eligible solutions will be assigned as $Rank=2$.

iii) Determine the $Rank$ index of each candidate solution in CP population according to the same dominance rule.

2) Cdis Index

The $Cdis$ index is usually used to evaluate the distribution of solution sets [15, 19]. In MOOPF problems, the candidate solutions with smaller $Rank$ index and larger $Cdis$ index are preferred. The way to calculate the $Cdis$ index is described as (26).

$$Cdis(Lo_i) = \sum_{j=1}^{Nc} \frac{O_j(Lo_{i-1}) - O_j(Lo_{i+1})}{O_j^{\max} - O_j^{\min}} \quad (26)$$

where $O_j(Lo_{i+1})$ is the value of the j th objective on the $(i+1)$ th individual. O_j^{\max} and O_j^{\min} are the maximum and minimum values of the j th objective.

According to the sorting rule defined as formulas (27) and (28), the CPNS strategy can pick out the top-ranked Nr solutions, which are the ultimate POS sets, from the CP population.

$$Rank(Lo_i) < Rank(Lo_j) \quad (27)$$

$$\begin{cases} Rank(Lo_i) = Rank(Lo_j) \\ Cdis(Lo_i) > Cdis(Lo_j) \end{cases} \quad (28)$$

D. MONBA-CPNS Method for MOOPF Problems

The main flow of solving MOOPF problems by the presented MONBA-CPNS algorithm is summarized in TABLE I.

TABLE I
Pseudo-code of MONBA-CPNS method on MOOPF problems

input: the parameters of MONBA-CPNS algorithm
Begin
Generate the initial IP and RP populations based on (25);
Update the position (D -dimensional control variables of power system) of each individual in initial CP population;
Calculate the values of objectives and constraints-violation by Newton Raphson method;
Determine the initial EP, NEP populations and the current Lo_{best} solution;
$ite=1$
while $ite < ite_{max}$ (the maximum iteration number)
if the i th individual belongs to the EP population
Update the position of the i th individual based on (21) and (17);
Carry out the Newton-Raphson power flow calculation;
Generate a random constant $rc1$ ($rc1 \in (0,1)$).
if $rc1 > pul_i$
Generate the Lo_{new} solution;
Generate another random constant $rc2$ ($rc2 \in (0,1)$);
if ($rc2 < lou_i$) && (Lo_{new} dominates Lo_{best})
$Lo_{best} = Lo_{new}$;
Update lou_i and pul_i based on (18) and (19);
end if
end if
if the j th individual belongs to the NEP population
Update the position of the j th individual: $Lo_j = Lo_n + \varphi * Lo_n$ (Lo_n is a random solution of EP population and $\varphi = 1 \times 10^{-6}$);
end if
Calculate the power flow for the renewed CP population;
Determine the current POS set based on the proposed CPNS strategy;
$ite=ite+1$;
end while
end
output: the final-selected POS set and Lo_{best} solution

IV. SYSTEMS AND TRIALS

Two tri-objective and four bi-objective trials are carried out the IEEE 30-node, IEEE 57-node and IEEE 118-node systems.

A. Parameters

Firstly, taking the simultaneous optimization of OF and OP an example, the influences of ite_{max} and population-size Nr on optimization quality are studied. This case is simulated on the IEEE 30-node system, whose structure and typical parameters can be found in [6, 21].

Fig.1 gives the Pareto Frontiers (PFs) with different ite_{max} obtained by MONBA-CPNS method and it indicates that the ite_{max} of 100 get the worst PF while the ite_{max} of 300 and 400 achieve the gratifying ones. Thus, the ite_{max} is set as $ite_{max}=300$ in this paper to save operation time. Fig.2 gives the PFs of MONBA-CPNS algorithm which shows that the presented method can find the well-distributed PFs in different-size populations. The population with 100 candidate solutions is employed in this paper.

B. Trials on IEEE 30-node system

Three multi-objective combinations are simulated on the IEEE 30-node system. To verify the applicability of MONBA-CPNS method, the NSGA-II and MOBBA-CPNS are adopted as comparison algorithms.

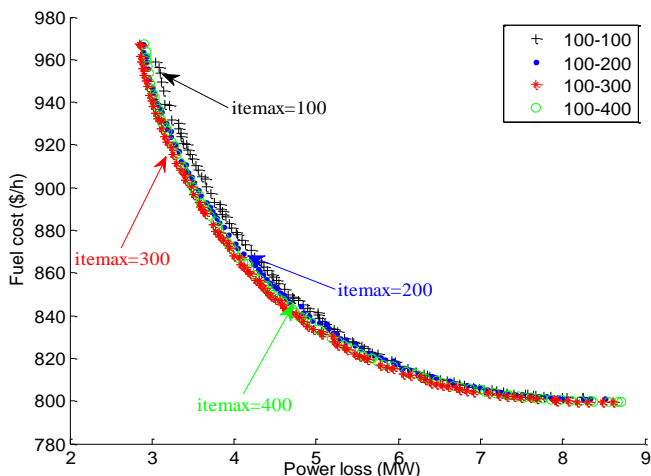


Fig.1 PFs with different ite_{max} ($Nr=100$)

1) Case1: Optimization of OP and OF

The case1 aims to optimize OP and OF at the same time on IEEE 30-node system. Fig.3 gives the PFs of case1 obtained by NSGA-II, MOBBA-CPNS and MONBA-CPNS methods. It clearly shows that MONBA-CPNS method achieves the evenly distributed PF, which is obviously superior to the two comparison algorithms. Besides, the distribution of two boundary solutions (BS1p and BS1f) found by MONBA-CPNS method and the BCS solutions found by three involved algorithms is shown in Fig.4. TABLE II gives the 24-dimensional control variables of obtained BCS solutions and the comparison results of other published literatures. It intuitively states that the BCS of MONBA-CPNS method with 4.9630 MW of OP and 833.6576 \$/h of OF dominates the BCSs of NSGA-II and MOBBA-CPNS methods. As a supplement, the BS1p solution includes minimal OP of 2.8426MW while the BS1f solution includes minimal OF of 799.4739 \$/h.

2) Case2: Optimization of OP and OF_v

The non-convex characteristic of valve-point effect makes it more difficult to solve the MOOPF problems. Fig.5 gives the PFs of case2 which aims to optimize OP and OF_v concurrently. It clearly states that the MOBBA-CPNS method can seek a preferable PF than NSGA-II method while the MONBA-CPNS method achieves the best one. In addition, TABLE III gives the specific control variables of three BCS solutions.

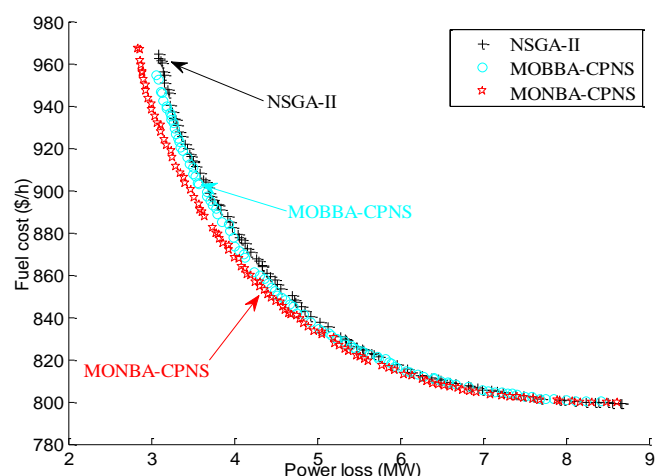


Fig.3 PFs of case1

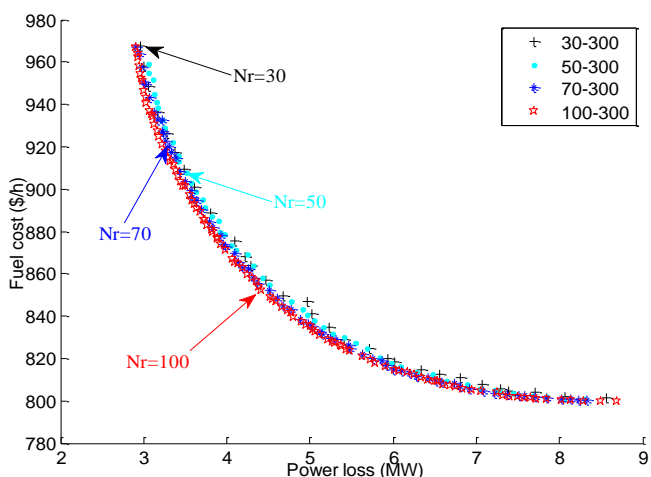


Fig.2 PFs with different-size population ($ite_{max}=300$)

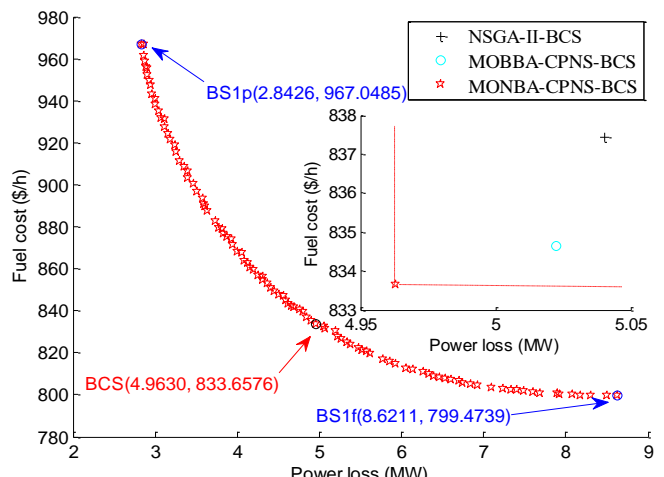


Fig.4 Special solutions of case1

TABLE II
Control variables and two comparison results of case1

control variables	NSGA-II	MOBBA-CPNS	MONBA-CPNS	MODFA [15]	NSGA-III [15]
P _{G2} (MW)	53.5094	52.1822	49.6735	54.2664	50.7171
P _{G5} (MW)	33.5644	32.7244	32.8900	31.6877	34.2440
P _{G8} (MW)	34.4545	35.0000	35.0000	34.9979	34.9912
P _{G11} (MW)	25.7106	26.9444	27.8501	29.6745	27.5983
P _{G13} (MW)	25.3576	23.7615	23.0504	20.4946	22.3721
V _{G1} (p.u.)	1.0991	1.1000	1.1000	1.0998	1.0791
V _{G2} (p.u.)	1.0886	1.0873	1.0906	1.0902	1.0677
V _{G5} (p.u.)	1.0649	1.0639	1.0687	1.0696	1.0428
V _{G8} (p.u.)	1.0741	1.0743	1.0808	1.0789	1.0497
V _{G11} (p.u.)	1.0609	1.1000	1.1000	1.0984	1.0997
V _{G13} (p.u.)	1.0890	1.0898	1.1000	1.0996	1.0902
T ₁₁ (p.u.)	1.0085	1.0193	1.0206	1.0376	0.9194
T ₁₂ (p.u.)	1.0089	0.9760	0.9335	0.9199	0.9955
T ₁₅ (p.u.)	1.0511	0.9834	0.9877	0.9820	0.9847
T ₃₆ (p.u.)	1.0028	0.9842	0.9668	0.9719	0.9648
Q _{C10} (p.u.)	0.0087	0.0404	0.0217	0.0494	0.0262
Q _{C12} (p.u.)	0.0135	0.0419	0.0500	0.0276	0.0496
Q _{C15} (p.u.)	0.0354	0.0131	0.0500	0.0488	0.0366
Q _{C17} (p.u.)	0.0241	0.0031	0.0464	0.0497	0.0035
Q _{C20} (p.u.)	0.0318	0.0111	0.0493	0.0367	0.0490
Q _{C21} (p.u.)	0.0072	0.0492	0.0500	0.0500	0.0216
Q _{C23} (p.u.)	0.0164	0.0409	0.0197	0.0458	0.0224
Q _{C24} (p.u.)	0.0347	0.0373	0.0500	0.0471	0.0123
Q _{C29} (p.u.)	0.0036	0.0408	0.0237	0.0204	0.0343
OF(\$/h)	837.4190	834.6417	833.6576	833.9365	836.8076
OP(MW)	5.0405	5.0223	4.9630	4.9561	5.1775

TABLE III shows the BCS of MONBA-CPNS method which includes 857.8741 \$/h of *OF_v* and 5.8954 MW of *OP* is obviously predominant than the BCS of two comparison methods. In contrast to the comparison results given in TABLE III, the superiority of MONBA-CPNS algorithm in finding higher-performance BCS solutions is verified.

3) Case3: Optimization of *OE*, *OP* and *OF*

The computational difficulty of tri-objective optimizations is obviously greater than that of the bi-objective ones. In case3, the *OE*, *OP* and *OF* are optimized simultaneously and Fig.6 gives the PFs of three methods. It can be observed clearly that three mentioned algorithms find uniformly distributed PFs while the MONBA-CPNS method obtains the most ideal one. Besides, TABLE IV gives the details of BCS solutions for case3. The BCS solution of innovative MONBA-CPNS method composed by 884.6227 \$/h of *OF*, 0.2043 ton/h of *OE* and 3.7791 MW of *OP* dominates the BCS solution of NSGA-II method.

C. Trials on IEEE 57-node system

Both bi-objective and tri-objective trials are simulated on the IEEE 57-node system whose structure and effective ranges of electrical equipment can be found in literatures [6, 15].

1) Case4: Optimization of *OP* and *OF*

Fig.7 gives the PFs of case4, which takes the simultaneous optimization of *OP* and *OF* goals, found by MONBA-CPNS and two comparison algorithms. It intuitively states that MONBA-CPNS method obtains the PF with more superior performance. Encouragingly, the advantages of proposed algorithm are more evident in the larger-scale IEEE 57-node system. Besides, Fig.8 shows the distribution of two boundary solutions (BS4p and BS4f) found by MONBA-CPNS algorithm and the BCS solutions found by three related algorithms. In great detail, the BS4p solution includes 9.9126 MW of minimal *OP* and 44678.5070 \$/h of *OF* while the

BS4f solution includes 14.8138 MW of *OP* and 41655.1801 \$/h of minimal *OF*.

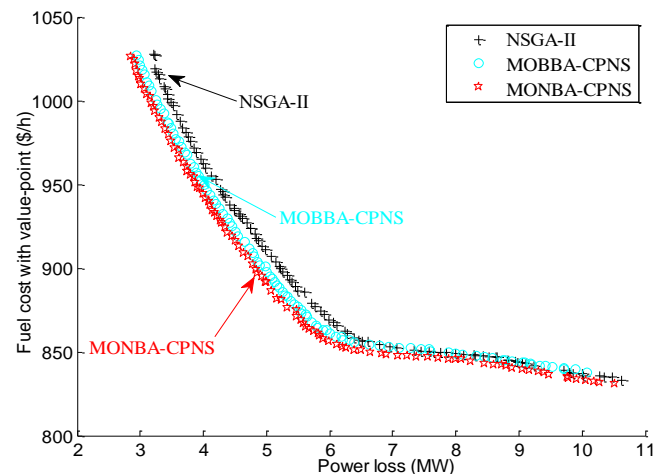


Fig.5 PFs of case2

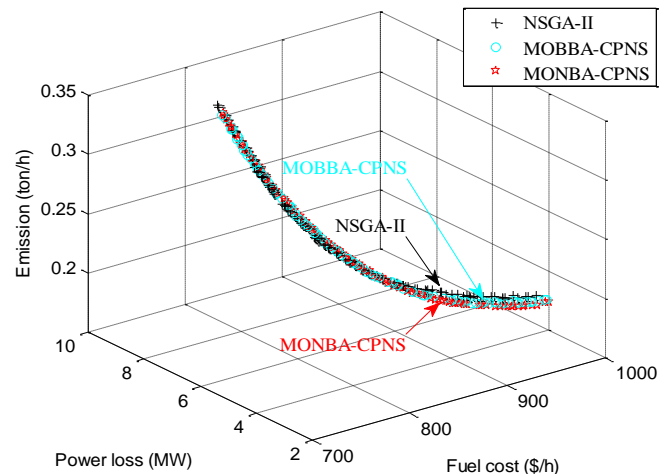


Fig.6 PFs of case3

TABLE III
Control variables and two comparison results of case2

control variables	NSGA-II	MOBBA-CPNS	MONBA-CPNS	MOFA-CPA[11]	MOFA-PFA[11]
P _{G2} (MW)	55.8345	51.3082	52.1270	53.613	49.098
P _{G5} (MW)	28.6866	27.3565	29.3173	30.305	29.139
P _{G8} (MW)	35.0000	32.2696	34.9819	34.428	35.000
P _{G11} (MW)	21.8390	26.2893	22.4170	22.187	23.853
P _{G13} (MW)	15.2409	15.5387	15.1392	13.928	17.249
V _{G1} (p.u.)	1.0669	1.09845	1.0984	1.1000	1.1000
V _{G2} (p.u.)	1.0534	1.0919	1.0882	1.0902	1.0923
V _{G5} (p.u.)	1.0331	1.0610	1.0655	1.0646	1.0631
V _{G8} (p.u.)	1.0393	1.0721	1.0774	1.0804	1.0811
V _{G11} (p.u.)	1.0879	1.0654	1.0979	1.1000	1.0714
V _{G13} (p.u.)	1.0868	1.0554	1.0995	1.1000	1.0422
T ₁₁ (p.u.)	0.9594	0.9841	1.0477	1.0210	1.0760
T ₁₂ (p.u.)	0.9624	1.0446	0.9528	0.9270	0.9850
T ₁₅ (p.u.)	0.9713	1.0183	0.9785	0.9870	1.0440
T ₃₆ (p.u.)	0.9469	1.0094	0.9699	0.9650	1.0110
Q _{C10} (p.u.)	0.0098	0.0143	0.0500	0.0230	0.0060
Q _{C12} (p.u.)	0.0428	0.0329	0.0329	0.0250	0.0140
Q _{C15} (p.u.)	0.0132	0.0307	0.0224	0.0320	0.0170
Q _{C17} (p.u.)	0.0170	0.0307	0.0500	0.0110	0.0310
Q _{C20} (p.u.)	0.0473	0.0458	0.0473	0.0350	0.0400
Q _{C21} (p.u.)	0.0255	0.0377	0.0500	0.0050	0.0100
Q _{C23} (p.u.)	0.0099	0.0412	0.0365	0.0330	0.0450
Q _{C24} (p.u.)	0.0403	0.0425	0.0338	0.0480	0.0250
Q _{C29} (p.u.)	0.0083	0.0341	0.0223	0.0140	0.0090
OF _i (\$/h)	860.8750	858.9543	857.8741	858.50	860.37
OP(MW)	6.2840	6.1070	5.8954	5.9031	5.9547

TABLE IV
Control variables of case3

control variables	NSGA-II	MOBBA-CPNS	MONBA-CPNS
P _{G2} (MW)	70.7600	69.5914	66.1336
P _{G5} (MW)	36.1766	38.8062	38.5071
P _{G8} (MW)	34.8281	34.1945	35.0000
P _{G11} (MW)	28.5770	30.0000	30.0000
P _{G13} (MW)	35.8675	33.6466	34.2665
V _{G1} (p.u.)	1.0567	1.0939	1.0994
V _{G2} (p.u.)	1.0498	1.0864	1.0916
V _{G5} (p.u.)	1.0293	1.0652	1.0760
V _{G8} (p.u.)	1.0411	1.0843	1.0805
V _{G11} (p.u.)	1.0618	1.0902	1.0906
V _{G13} (p.u.)	1.0455	1.0895	1.0998
T ₁₁ (p.u.)	0.9765	0.9953	1.0314
T ₁₂ (p.u.)	0.9335	1.0041	0.9246
T ₁₅ (p.u.)	1.0927	1.0528	0.9976
T ₃₆ (p.u.)	0.9764	1.0226	0.9695
Q _{C10} (p.u.)	0.0332	0.0035	0.0500
Q _{C12} (p.u.)	0.0016	0.0138	0.0306
Q _{C15} (p.u.)	0.0415	0.0465	0.0466
Q _{C17} (p.u.)	0.0424	0.0199	0.0500
Q _{C20} (p.u.)	0.0409	0.0262	0.0449
Q _{C21} (p.u.)	0.0303	0.0441	0.0259
Q _{C23} (p.u.)	0.0126	0.0142	0.0353
Q _{C24} (p.u.)	0.0065	0.0483	0.0486
Q _{C29} (p.u.)	0.0265	0.0308	0.0177
OF(\$/h)	887.0202	888.8314	884.6227
OE(ton/h)	0.2046	0.2039	0.2043
OP(MW)	4.4881	3.8920	3.7791

Meanwhile, TABLE V gives the 33-dimensional control variables of obtained BCS solutions and the comparison result of other published literature. It is not difficult to find that the BCS solution of MONBA-CPNS method which consists by 42085.4288 \$/h of OF and 10.8400 MW of OP dominates the two BCS solutions obtained by other methods.

2) Case5: Optimization of OP, OE and OF

Three objectives of OP, OE and OF are optimized at the same time on the IEEE 57-node system. Fig.9 and Fig. 10 give the comparison results of MONBA-CPNS algorithm with NSGA-II and MOBBA-CPNS algorithms, respectively. It

shows that the NSGA-II method obtains a more densely distributed PF and MONBA-CPNS method achieves a more advantageous PF than MOBBA-CPNS. In addition, TABLE VI gives the accurate control variables of case5.

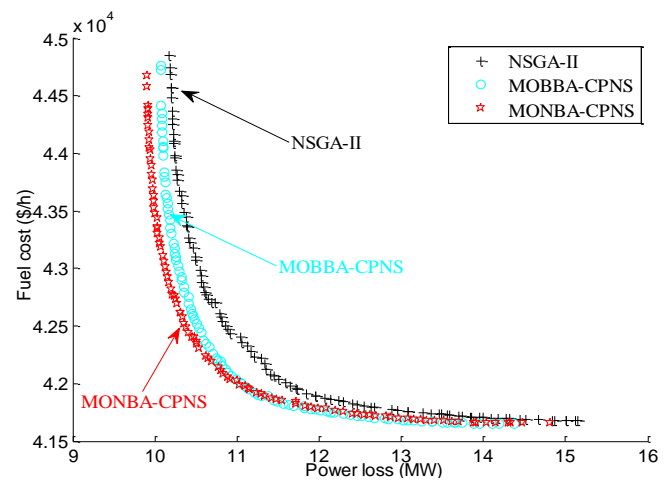


Fig.7 PFs of case4

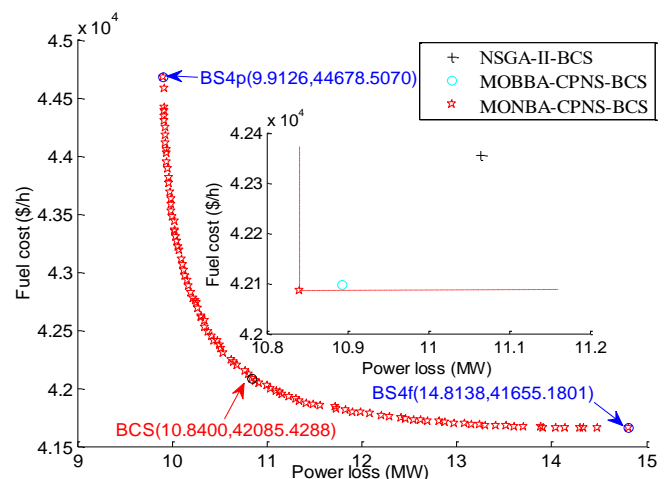


Fig.8 Special solutions of case4

TABLE V
Control variables and comparison result of case4

control variables	NSGA-II	MOBBA-CPNS	MONBA-CPNS	MOIBA [6]
PG2(MW)	48.0893	72.0732	60.8427	53.4086
PG3(MW)	74.2743	67.8187	62.8562	62.6900
PG6(MW)	99.7293	58.5408	89.1136	89.8593
PG8(MW)	358.1706	385.4722	372.8222	377.9932
PG9(MW)	99.9864	98.7976	99.9507	99.9232
PG12(MW)	409.7494	410.0000	409.7755	410.0000
VG1(p.u.)	1.0132	1.0961	1.0680	1.0536
VG2(p.u.)	1.0089	1.0939	1.0652	1.0467
VG3(p.u.)	1.0138	1.0915	1.0656	1.0436
VG6(p.u.)	1.0305	1.0942	1.0785	1.0521
VG8(p.u.)	1.0425	1.0999	1.0815	1.0613
VG9(p.u.)	1.0275	1.0911	1.073	1.0481
VG12(p.u.)	1.0189	1.0704	1.0585	1.0337
T19(p.u.)	0.9765	1.0639	1.0504	1.0350
T20(p.u.)	1.0536	1.0554	0.9934	0.9496
T31(p.u.)	1.0540	1.0480	0.9811	0.9837
T35(p.u.)	1.0215	1.0914	0.9660	1.0267
T36(p.u.)	1.0888	0.9475	1.0410	1.0055
T37(p.u.)	0.9938	1.0366	1.0166	1.0597
T41(p.u.)	0.9341	1.0250	0.9897	0.9682
T46(p.u.)	0.9769	0.9783	0.9303	0.9558
T54(p.u.)	0.9064	0.9933	0.9341	0.9893
T58(p.u.)	0.9250	0.9763	0.9949	0.9281
T59(p.u.)	0.9275	0.9662	0.9818	0.9192
T65(p.u.)	0.9429	0.9819	0.9824	0.9525
T66(p.u.)	0.9034	0.9535	0.9615	0.9441
T71(p.u.)	0.9227	1.0498	0.9503	0.9527
T73(p.u.)	0.9872	1.0469	0.9495	0.9421
T76(p.u.)	0.9594	1.0603	0.9855	1.0606
T80(p.u.)	0.9487	1.0361	0.9773	0.9688
QC18(p.u.)	0.2231	0.0379	0.2248	0.2343
QC25(p.u.)	0.1605	0.1599	0.1509	0.1310
QC53(p.u.)	0.1383	0.1019	0.1449	0.1876
OF (\$/h)	42353.3990	42095.8591	42085.4288	42098.7213
OP(MW)	11.0646	10.8939	10.8400	11.4759

TABLE VI
Control variables of case5

variables	NSGA-II	MOBBA-CPNS	MONBA-CPNS
PG2(MW)	52.5225	93.6293	99.1093
PG3(MW)	119.9929	119.2268	97.7004
PG6(MW)	90.1155	93.6531	89.4406
PG8(MW)	314.9157	298.6863	312.8840
PG9(MW)	99.9551	99.3182	98.3716
PG12(MW)	393.7500	392.6745	404.5135
VG1(p.u.)	1.0708	1.0940	1.0940
VG2(p.u.)	1.0608	1.0926	1.0894
VG3(p.u.)	1.0438	1.0894	1.0883
VG6(p.u.)	1.0303	1.0899	1.0961
VG8(p.u.)	1.0249	1.0941	1.0980
VG9(p.u.)	1.0293	1.0930	1.0893
VG12(p.u.)	1.0348	1.0861	1.0830
T19(p.u.)	0.9115	1.0179	0.9756
T20(p.u.)	0.9706	1.0835	1.0194
T31(p.u.)	1.0338	1.0190	0.9533
T35(p.u.)	1.0472	0.9972	1.1000
T36(p.u.)	1.0978	0.9958	1.0631
T37(p.u.)	1.0522	1.0169	0.9934
T41(p.u.)	0.9216	1.0081	1.0238
T46(p.u.)	1.0156	0.9802	0.9594
T54(p.u.)	0.9020	0.9048	0.9938
T58(p.u.)	0.9360	0.9912	0.9738
T59(p.u.)	0.9571	0.9777	0.9791
T65(p.u.)	0.9277	0.9841	0.9907
T66(p.u.)	0.9057	0.9425	0.9709
T71(p.u.)	1.0070	1.0269	1.0038
T73(p.u.)	1.0522	1.0690	1.0997
T76(p.u.)	1.0067	0.9562	0.9763
T80(p.u.)	0.9463	1.0082	1.0077
QC18(p.u.)	0.0989	0.1974	0.1225
QC25(p.u.)	0.1685	0.1145	0.2179
QC53(p.u.)	0.0898	0.1211	0.1676
OF (\$/h)	43931.3028	43834.7089	43052.1824
OE (ton/h)	1.4327	1.3559	1.4292
OP(MW)	11.2676	10.5660	10.5961

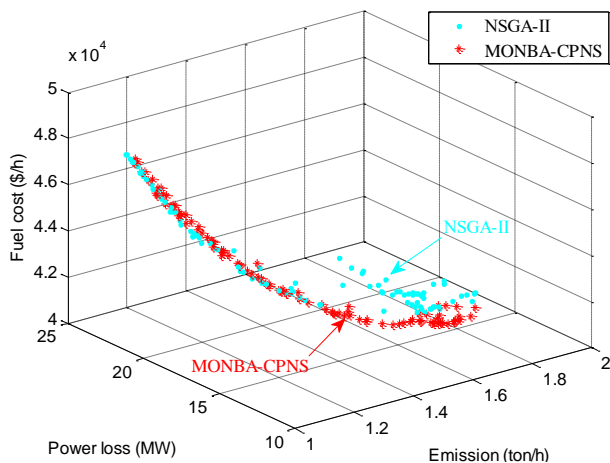


Fig.9 PFs of NSGA-II and MONBA-CPNS for case5

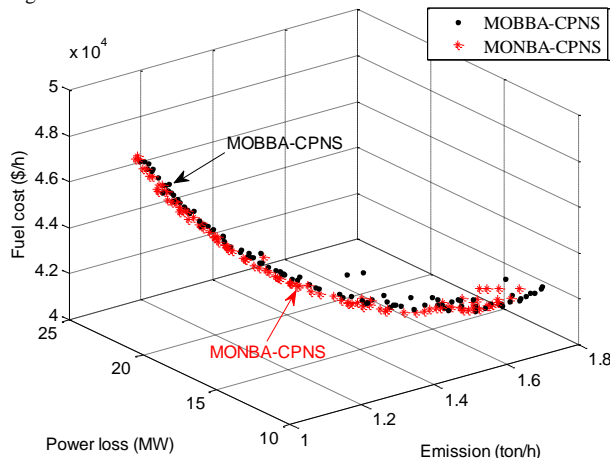


Fig.10 PFs of MOBBA-CPNS and MONBA-CPNS for case5

TABLE VI indicates that the BCS of MONBA-CPNS method with 43052.1824 \$/h of *OF*, 1.4292 ton/h of *OE* and 10.5961 MW of *OP* is more desirable than the one of NSGA-II method. Although the BCS of MONBA-CPNS algorithm cannot directly dominate the BCS of MOBBA-CPNS algorithm, the PF obtained by the former method is indeed more valuable than that obtained by the latter in terms of distribution. It is worth noting that in order to guarantee the good optimization performance, the ite_{max} of case5 is selected as 500.

D. Trials on IEEE 118-node system

In case6, a bi-objective MOOPF case which optimizes *OP* and *OF* at the same time is simulated on the complex IEEE 118-node system. The details of IEEE 118-node system are clarified in literature [15]. Fig. 11 gives the PFs obtained by three methods and it visually denotes that the suggested MONBA-CPNS algorithm has absolute advantages to achieve the PFs with favorable distribution and diversity, especially on the IEEE 118-node system with complex-structure and large-scale. Furthermore, Fig.12 reveals the distribution of special solutions for case6. Besides, TABLE VII gives the details of BCS solutions, the boundary solution with minimal *OP* (BS6p) and the boundary one with minimal *OF* (BS6f). Among them, the BCS of MONBA-CPNS method, which consists by 44.4002 MW of *OP* and 57647.7158 \$/h of *OF*, is obvious better than the ones found by NSGA-II and MOBBA-CPNS methods. It is worth pointing out that, the efficient MONBA-CPNS method is capable to obtain 33.9667 MW of minimal *OP* and 56370.4783 \$/h of minimal *OF*.

As a supplement, the parameter-settings of NSGA-II, MOBBA-CPNS and MONBA-CPNS algorithms are clarified in TABLE VIII.

V. EVALUATION

The computational complexity of three algorithms is measured based on the program runtime. The distribution and convergence of obtained POS are measured based on the SP and GD indicators.

A. Computation complexity

The computation complexity, which can be represented by running time, is used to evaluate the performance of modified MONBA-CPNS algorithm. An efficient algorithm should shorten the search time as much as possible without affecting optimization quality. The average running time of six simulation cases is listed in TABLE IX. Although it requires more running time than NSGA-II method, the proposed MONBA-CPNS algorithm does reduce the computational complexity than MOBBA-CPNS algorithm and achieves the more superior performance in solving MOOPF problems.

B. Evaluation indicators

The SP and GD indexes are employed to assess the distribution and the convergence of obtained POS set quantitatively. Thirty independent experimental results of four bi-objective cases (case1~case2, case4 and case6) involved in this paper are analyzed with the above two indicators.

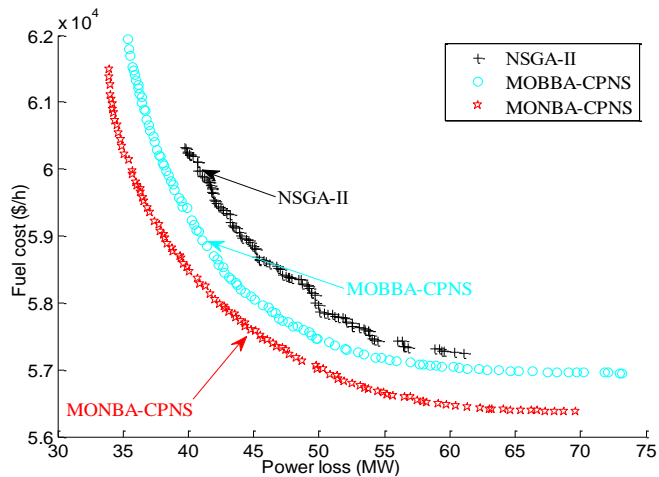


Fig.11 PFs of case6

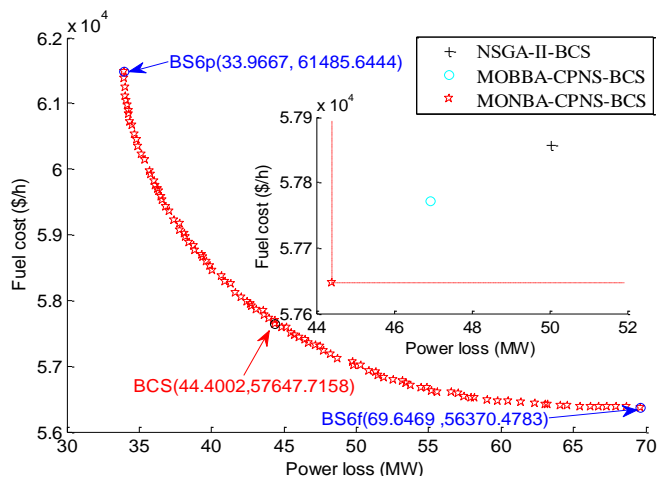


Fig.12 Special solutions of case6

1) SP

The SP index defined as (29) is used to evaluate the distribution of POS set by calculating the variance range of neighboring vectors. The meaning of specific symbols and the application of SP index are clarified in literatures [15, 22-24]. The SP=0 represents that all power flow solutions of the current PF are spaced equidistantly.

$$SP = \sqrt{\frac{1}{Nr-1} \sum_{i=1}^{Nr} \left(\frac{1}{Nr} \sum_{i=1}^{Nr} d_i - d_i \right)^2} \quad (29)$$

$$d_i = \min_{j=1,2,\dots,Nr} \left(\sum_{k=1}^M |O_k^i - O_k^j| \right) \quad (30)$$

The boxplot, which gives a visual representation of median value and outliers, is a predominant computer technique to conduct data analysis [25]. The boxplots of SP index are shown in Fig.13 while TABLE X gives the average and standard deviation of SP indicator. It shows that compared with NSGA-II method, MONBA-CPNS method achieves similar or even better performance for case1 and case2. In case4 and case6, MONBA-CPNS method has minimal deviation and fewer outliers which state that the modified MONBA-CPNS algorithm obtains better consistent results in 30 independent trials. In general, the uniform-distribution of POS set obtained by the MONBA-CPNS algorithm still has some room for improvement.

TABLE VII
Special solutions of case6

	NSGA-II		MOBBA-CPNS		MONBA-CPNS	
	OP(MW)	OF(\$/h)	OP(MW)	OF(\$/h)	OP(MW)	OF(\$/h)
BCS	50.0451	57856.6500	46.9449	57771.1082	44.4002	57647.7158
BS6f	61.0544	57247.3526	73.1888	56950.4687	69.64698	56370.4783
BS6p	39.7004	60318.4619	35.3389	61942.4076	33.9667	61485.6444

TABLE VIII
Parameter-settings for testing cases

Algorithms	Parameters	Cases	
		300 (case1-case4)	500 (case5-case6)
Common parameters	ite_{max}	300 (case1-case4)	500 (case5-case6)
	IP size		100
	RP size		100
NSGA-II	mutation index/percentage		20/1
	crossover index/percentage		20/0.1
MOBBA-CPNS	Fr_{min}/Fr_{max}		0/2
	lou		0.95
	$pulo$		0.5
	l_1/l_2		0.9/0.9
MONBA-CPNS	Fr_{min}/Fr_{max}		0/2
	lou		0.95
	$pulo$		0.5
	l_1/l_2		0.9/0.9
	We_{min}/We_{max}		0.4/0.9

TABLE IX
Average running time (sec)

Algorithm	case1	case2	case3	case4	case5	case6
NSGA-II	197.56	195.46	198.34	314.71	519.02	1730.55
MOBBA-CPNS	216.64	223.39	224.33	326.03	535.20	1796.42
MONBA-CPNS	212.47	206.76	204.01	319.40	527.42	1745.22

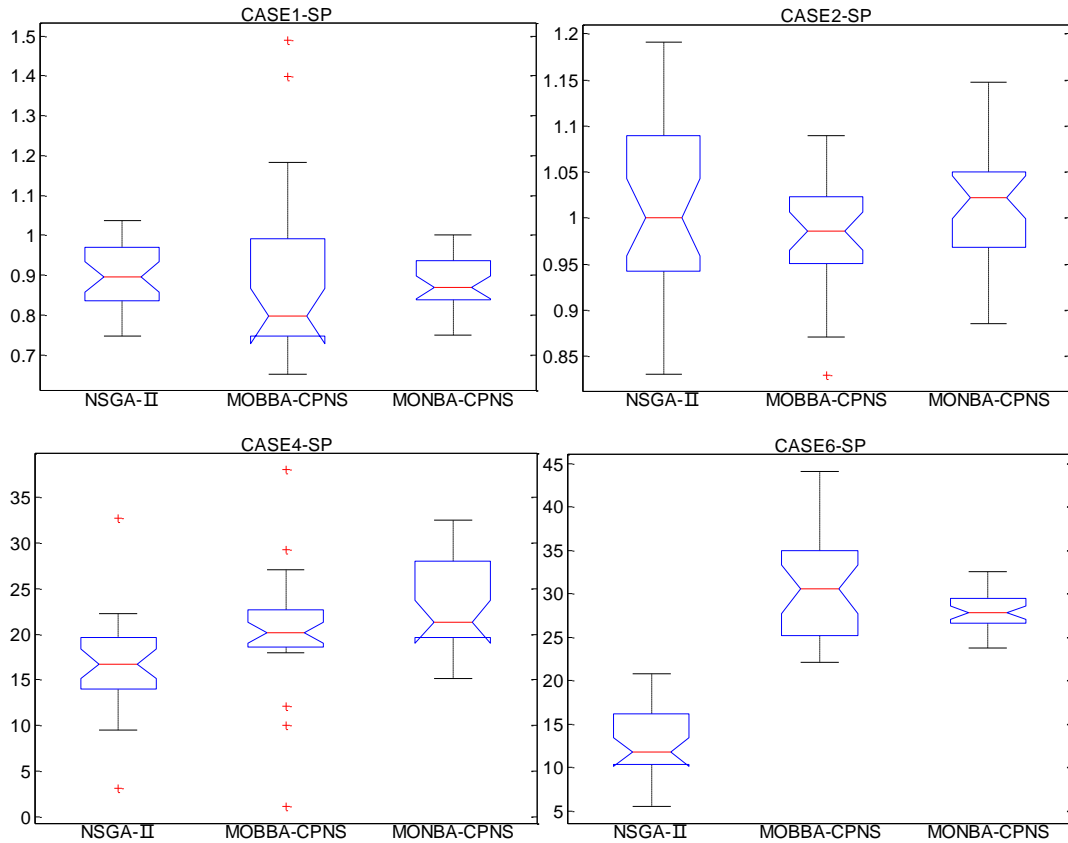


Fig.13 SP index of four bi-objective cases

2) *GD*

The *GD* index defined as (31) can evaluate the convergence of obtained PF to the real one. The application of *GD* index can be referred to literatures [15, 26]. The *GD*=0 represents that all power flow solutions of obtained PF are completely consistent with the real PF.

$$GD = \frac{\sqrt{\sum_{i=1}^{Nr} Ed_i^2}}{Nr} \quad (31)$$

where *Ed* is the Euclidean distance between the *i*th power flow solution of current POS set and the nearest one of the real

PF.

Fig.14 shows the boxplots and TABLE XI gives the average and standard deviation of *GD* index. It clearly denotes that MONBA-CPNS algorithm, which achieves the smallest average value of *GD* index, determines the high-quality PFs which are more in conformity with the real one. Except in case4, MONBA-CPNS algorithm achieves the minimal deviation value and it shows that this proposed method has more advantageous stability in handling MOOPF problems.

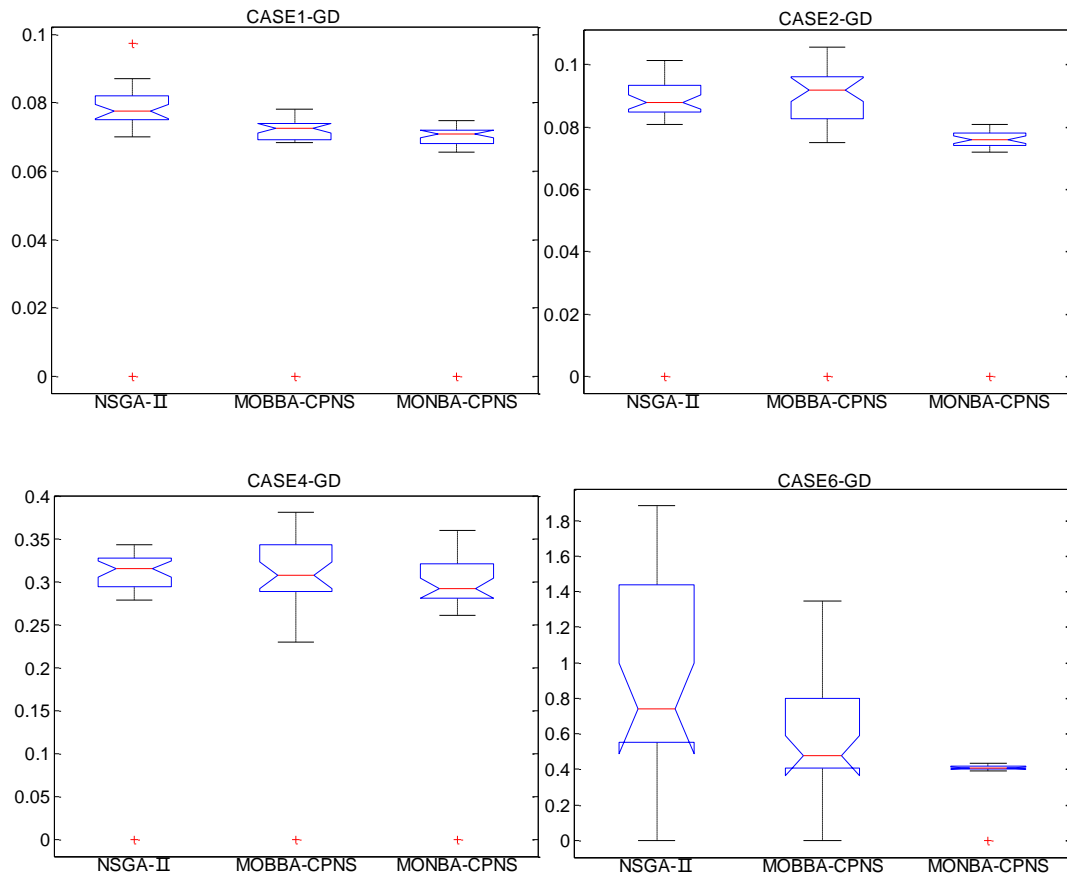


Fig.14 *GD* index of four bi-objective cases

TABLE X
Details of SP index

Evaluation index	NSGA-II		MOBBA-CPNS		MONBA-CPNS		
	mean	deviation	mean	deviation	mean	deviation	
SP	case1	0.8965	0.0820	0.8815	0.2101	0.8805	0.0675
	case2	1.0143	0.0903	0.9839	0.0599	1.0137	0.0677
	case4	16.6332	5.0586	20.5272	6.1758	23.0513	4.7478
	case6	12.9179	4.0372	30.4938	5.6418	27.9470	2.1125

TABLE XI
Details of *GD* index

Evaluation index	NSGA-II		MOBBA-CPNS		MONBA-CPNS		
	mean	deviation	mean	deviation	mean	deviation	
GD	case1	0.0758	0.0154	0.0699	0.0135	0.0681	0.0131
	case2	0.0863	0.0171	0.0880	0.0186	0.0737	0.0141
	case4	0.3032	0.0602	0.3033	0.0660	0.2903	0.0604
	case6	0.9465	0.5103	0.6128	0.3241	0.3960	0.0755

VI. CONCLUSION

In order to deal with the MOOPF problems more effectively and realize the economic operation of power systems, an innovative MONBA-CPNS method is proposed in this paper. The MONBA-CPNS method combines the MONBA algorithm to improve global search efficiency and the CPNS sorting strategy to seek POS set with superior convergence. Six MOOPF trials which are carried out on the IEEE 30-node, 57-node and 118-node systems powerfully verify the effectiveness and superiority of the presented MONBA-CPNS algorithm. The detailed experimental results including evaluation analysis based on SP and GD evaluation indexes demonstrate that the MONBA-CPNS algorithm provides a novel and efficient way to solve the complex MOOPF problems.

ACKNOWLEDGEMENTS

The authors would like to thank the editors and reviewers for their constructive comments and valuable suggestions.

REFERENCES

- [1] S. Duman, "A Modified Moth Swarm Algorithm Based on an Arithmetic Crossover for Constrained Optimization and Optimal Power Flow Problems", *IEEE Access*, vol. 6, pp. 45394-45416, 2018.
- [2] T. T. Nguyen, "A high performance social spider optimization algorithm for optimal power flow solution with single objective optimization", *Energy*, vol. 171, pp. 218-240, 2019.
- [3] K. Y. Chan, G. T. Y. Pong and K. W. Chan, "Investigation of Hybrid Particle Swarm Optimization Methods for Solving Transient-Stability Constrained Optimal Power Flow Problems", *Engineering Letters*, vol. 16, no. 1, pp. 61-67, 2008.
- [4] G. Chen, Z. Lu and Z. Zhang, "Improved Krill Herd Algorithm with Novel Constraint Handling Method for Solving Optimal Power Flow Problems", *Energies*, vol. 11, no. 1, pp. 76, 2018.
- [5] Y. Yuan, X. Wu, P. Wang, and X. Yuan, "Application of improved bat algorithm in optimal power flow problem", *Applied Intelligence*, vol. 48, no. 8, pp. 2304-2314, 2018.
- [6] G. Chen, J. Qian, Z. Zhang, and Z. Sun, "Multi-objective Improved Bat Algorithm for Optimizing Fuel Cost, Emission and Active Power Loss in Power System", *IAENG International Journal of Computer Science*, vol. 46, no. 1, pp. 118-133, 2019.
- [7] J. Zhang, S. Wang, Q. Tang, Y. Zhou, and T. Zeng, "An improved NSGA-III integrating adaptive elimination strategy to solution of many-objective optimal power flow problems", *Energy*, vol. 172, pp. 945-957, 2019.
- [8] G. Chen, S. Qiu, Z. Zhang, and Z. Sun, "Quasi-oppositional cuckoo search algorithm for multi-objective optimal power flow", *IAENG International Journal of Computer Science*, vol. 45, no. 2, pp. 255-266, 2018.
- [9] E. Barocio, J. Regalado, E. Cuevas, F. Uribe, P. Zuniga, and P. J. Ramirez Torres, "Modified bio-inspired optimisation algorithm with a centroid decision making approach for solving a multi-objective optimal power flow problem", *IET Generation Transmission & Distribution*, vol. 11, no. 4, pp. 1012-1022, 2017.
- [10] W. Warid, H. Hizam, N. Mariun, and N. I. A. Wahab, "A novel quasi-oppositional modified Jaya algorithm for multi-objective optimal power flow solution", *Applied Soft Computing*, vol. 65, pp. 360-373, 2018.
- [11] G. Chen, X. Yi, Z. Zhang, and H. Lei, "Solving the Multi-Objective Optimal Power Flow Problem Using the Multi-Objective Firefly Algorithm with a Constraints-Prior Pareto-Domination Approach", *Energies*, vol. 11, no. 12, pp. 3438, 2018.
- [12] L. Zhu and J. Wang, "Data clustering method based on bat algorithm and parameters optimization", *Engineering Letters*, vol. 27, no. 1, pp. 241-250, 2019.
- [13] E. Osaba, X. Yang, Jr. I. Fister, J. Del Ser, P. Lopez-Garcia, and A. J. Vazquez-Pardavila, "A Discrete and Improved Bat Algorithm for solving a medical goods distribution problem with pharmacological waste collection", *Swarm and Evolutionary Computation*, vol. 44, pp. 273-286, 2019.
- [14] C. K. Ng, C. H. Wu, W. H. Ip, and L. Y. Kai, "A Smart Bat Algorithm for Wireless Sensor Network Deployment in 3-D Environment", *IEEE Communications Letters*, vol. 22, no. 10, pp. 2120-2123, 2018.
- [15] G. Chen, X. Yi, Z. Zhang, and H. Wang, "Applications of multi-objective dimension-based firefly algorithm to optimize the power losses, emission, and cost in power systems", *Applied Soft Computing*, vol. 68, pp. 322-342, 2018.
- [16] S. Khunkitti, A. Siritaratiwat, S. Premrudeepreechacharn, R. Chatthaworn, and N. R. Watson, "A Hybrid DA-PSO Optimization Algorithm for Multiobjective Optimal Power Flow Problems", *Energies*, vol. 11, no. 9, pp. 2270, 2018.
- [17] X. Yang, "Bat algorithm for multi-objective optimisation", *International Journal of Bio-Inspired Computation*, vol. 3, no. 5, pp. 267-274, 2011.
- [18] M. A. Al-Betar, M. A. Awadallah, H. Faris, X. Yang, A. Tajudin Khader, and O. A. Alomari, "Bat-inspired algorithms with natural selection mechanisms for global optimization", *Neurocomputing*, vol. 273, pp. 448-465, 2018.
- [19] K. Deb, A. Pratap, S. Agarwal, and T. Meyarivan, "A fast and elitist multiobjective genetic algorithm: NSGA-II", *IEEE Transactions on Evolutionary Computation*, vol. 6, pp. 182-197, 2002.
- [20] O. T. Altinoz, K. Deb and A. E. Yilmaz, "Evaluation of the migrated solutions for distributing reference point-based multi-objective optimization algorithms", *Information Sciences*, vol. 467, pp. 750-765, 2018.
- [21] G. Chen, S. Qiu, Z. Zhang, Z. Sun, and H. Liao, "Optimal Power Flow Using Gbest-Guided Cuckoo Search Algorithm with Feedback Control Strategy and Constraint Domination Rule", *Mathematical Problems in Engineering*, vol. 2, pp. 1-14, 2017.
- [22] F. S. Lobato, M. N. Sousa, M. A. Silva, and A. R. Machado, "Multi-objective optimization and bio-inspired methods applied to machinability of stainless steel", *Applied Soft Computing*, vol. 22, pp. 261-271, 2014.
- [23] R. Gan, Y. Guo, J. Zheng, J. Zou, and S. Yang, "The Effect of Diversity Maintenance on Prediction in Dynamic Multi-objective Optimization", *Applied Soft Computing*, vol. 58, pp. 631-647, 2017.
- [24] D. Tao, L. Cheng, F. Li, T. Chen, and R. Liu, "A bi-objective DC-optimal power flow model using linear relaxation-based second order cone programming and its Pareto Frontier", *International Journal of Electrical Power & Energy Systems*, vol. 88, pp. 13-20, 2017.
- [25] M. Gertz and J. Krieter, "About the classification of abattoir data by using the boxplot-methodology and its derivatives", *Zuchtingkunde*, vol. 89, no. 6, pp. 401-412, 2017.
- [26] G. Chen, J. Qian, Z. Zhang, and Z. Sun, "Applications of Novel Hybrid Bat Algorithm With Constrained Pareto Fuzzy Dominant Rule on Multi-Objective Optimal Power Flow Problems", *IEEE Access*, vol. 7, no. 1, pp. 52060-52084, 2019.